ELSEVIER

Journal of Molecular Catalysis B: Enzymatic 18 (2002) 39–48

JOURNAL OF MOLECULAR CATALYSIS B: ENZYMATIC

www.elsevier.com/locate/molcatb

Oxidation of ABTS by hydrogen peroxide catalyzed by horseradish peroxidase encapsulated into sol–gel glass. Effects of glass matrix on reactivity

Ekaterina N. Kadnikova, Nenad M. Kostić*

Department of Chemistry, Iowa State University, Ames, IA 50011-3111, USA

Received 18 September 2001; received in revised form 28 December 2001; accepted 28 February 2002

Abstract

Encapsulation of horseradish peroxidase (HRP) by the sol–gel method into silica (SiO_2) or alkylated silica ($RSiO_2$, in which R is Me or Pr) yields biocatalytic glasses designated HRP@SiO_2 and HRP@$RSiO_2$. These new enzyme composite materials catalyze one-electron oxidation by H_2O_2 of the dye 2,2′-azino-bis(3-ethylbenzothiazoline-6-sulfonate) (ABTS) into the radical cation $ABTS^{\bullet+}$. In the presence of excess H_2O_2, $ABTS^{\bullet+}$ is converted into a mixture of at least five compounds. This undesirable side-reaction can be suppressed by using stoichiometric amount of H_2O_2. The effects of ABTS concentration and ionic strength of the buffer on the $ABTS^{\bullet+}$ yield and the apparent rate constant were investigated. The catalyst HRP@$MeSiO_2$ achieves higher $ABTS^{\bullet+}$ yields (70–85%) than HRP@SiO_2 and HRP@$PrSiO_2$ (30–40%) do. The apparent rate constants for HRP@$MeSiO_2$ are 7–10 times higher than those for HRP@SiO_2 and HRP@$PrSiO_2$. When the ionic strength of the buffer is raised, the rate constants increase for HRP@SiO_2 and HRP@$PrSiO_2$, and do not change for HRP@$MeSiO_2$. The diminished electrostatic interaction between the negatively-charged substrate, ABTS, and the surface of methylated silica is the main cause for the increased catalytic efficiency. These results are important for understanding of encapsulated and otherwise immobilized enzymes. The possible electrostatic effects should be taken into consideration in the choice of the matrix materials used in the design of biosensors, supported catalysts, and other composite materials.

Keywords: Sol–gel method; Horseradish peroxidase; ABTS

1. Introduction

Glasses made of silica and its various organic derivatives may be prepared at room temperature by the sol–gel method, i.e. by condensation–polymerization of suitable alkoxides [1]. Much attention has recently been devoted to the development of the sol–gel methods for encapsulation of biomolecules. Achievements in these studies opened many possibilities for basic and applied research in materials science, bioanalytical chemistry, biocatalysis, biotechnology, and environmental technology.

Research in our [2–9] and other [10–12] laboratories has shown, however, that enzymes and even small molecules may behave differently when free in solutions and when immobilized. More basic research is needed before supported catalysts, biosensors, and other composite materials can be turned into practical chemical devices.

In this work, we compare the catalytic performance of horseradish peroxidase (HRP) encapsulated

* Corresponding author. Tel.: +1-515-294-7715; fax: +1-515-294-0105.
E-mail address: nenad@iastate.edu (N.M. Kostić).

1381-1177/02/$ – see front matter © 2002 Elsevier Science B.V. All rights reserved.
PII: S1381-1177(02)00057-7

into different sol–gel glasses. We chose a known peroxidase-catalyzed reaction [13], one-electron oxidation of 2,2′-azino-bis(3-ethylbenzothiazoline-6-sulfonate) (ABTS), into the corresponding radical–cation, $ABTS^{\bullet+}$; see Eq. (1).

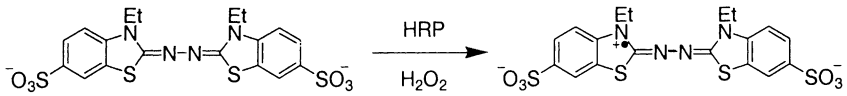

(1)

2. Experimental procedures

2.1. Chemicals

HRP was obtained from Sigma Chemical Co. Tetramethylorthosilicate (tetramethoxysilane), trimethoxypropylsilane, *iso*-butyltrimethoxysilane, poly(vinyl alcohol), diammonium salt of ABTS, and deuteriated water were obtained from Aldrich Chemical Co. Methyltrimethoxysilane was obtained from Strem Chemicals. Hexyltrimethoxysilane was obtained from Gelest Inc. Monosodium phosphate, disodium phosphate, sodium chloride, sodium fluoride, sodium hydroxide, ammonium persulfate, concentrated hydrochloric acid, and 3% aqueous hydrogen peroxide were obtained from Fisher Scientific Co. Distilled water was demineralized to electrical resistivity greater than 17 MΩ cm. Concentrations of ABTS ($\varepsilon_{340} = 36{,}000\,M^{-1}\,cm^{-1}$) and H_2O_2 ($\varepsilon_{240} = 39.4\,M^{-1}\,cm^{-1}$) in stock solutions were determined by ultraviolet–visible (UV–VIS) measurements.

2.2. Instruments

Elemental analyses were done with a Perkin-Elmer Model 2400 Series II instrument. AD-4 ultramicrobalance was used for weighing catalyst with 0.001 mg precision. UV–VIS spectra were recorded with a Perkin-Elmer Lambda 18 spectrophotometer. The components of the mixtures resulting from over-oxidation of ABTS were separated by a Hewlett Packard 1100 HPLC system containing an autosampler and a multiwavelength detector set at 215 and 280 nm. A Supelco Discovery C-18 column (25 cm × 4.6 mm, 5 μm) was used for the analytical runs, and a Vydac C-18 column 218TP101522 was used for the preparative runs. The eluting solvent A was 0.1% (v/v) trifluoroacetic acid in water, and solvent B was 0.08% (v/v) trifluoroacetic acid in acetonitrile. After the injection of the sample, the fraction of solvent B in eluent was kept at 0% for 5 min, and then it was linearly raised to 45% over a 35-min period. The flow rates were 1.0 and 10 ml min^{-1}, respectively, for analytical and preparative separations. Nuclear magnetic resonance (NMR) spectra were recorded with a Bruker DRX-400 spectrometer. Electrospray ionization–mass spectral (ESI–MS) analyses were performed on a Finnigan TSQ 700 triple quadrupole mass spectrometer fitted with a Finnigan ESI interface. Samples were introduced into the electrospray interface through an untreated fused-silica capillary (internal and external diameters of 50 and 190 μm, respectively). A mixture of myoglobin and the tetrapeptide Met–Arg–Phe–Ala was used for tuning and routine calibration of the instrument. A Harvard Apparatus syringe pump model 22 was used to introduce analytes into the mass spectrometer at a rate of 3 μl min^{-1}.

2.3. Encapsulation of horseradish peroxidase in sol–gel silica glass

A modification of a published method [1] was used. Aqueous HRP (1.25 mM, 1.00 ml), aqueous sodium fluoride (1.00 M, 0.200 ml), and aqueous poly(vinyl alcohol) (4% w/w, 0.400 ml) were combined with 0.128 ml of water. While the mixture was vigorously stirred with a vortex shaker, tetramethylorthosilicate (1.827 g, 12 mmol) was added. After ca. 10 s, when the mixture turned into a clear homogeneous solution and warmed up, it was placed into an ice bath. The gelation occurred ca. 10 s later, and the mixture was kept in the ice bath for 5 min. The sealed reaction vessel was kept at room temperature for 24 h and then opened. The gel was air-dried at 40 °C for 4 days. The resulting glass was ground in a mortar, and the powder was shaken with 10.0 ml of water at room temperature for 2 h. The solid was filtered off; washed with water, acetone, and hexane; and dried for 12 h at 40 °C. The

final product, designated HRP@SiO_2, was a beige powder. Elemental analysis found 3.39% C, 1.04% H, and 0.633% N, corresponding to 0.905 μmol HRP per gram of solid.

2.4. Encapsulation of horseradish peroxidase in sol–gel organosilica glass

Alkyltrimethoxysilane (12 mmol) was used instead of tetramethylorthosilicate in a procedure analogous to the one described above. The enzyme encapsulated in methylated silica glass, designated HRP@$MeSiO_2$, was obtained using 1.6346 g of methyltrimethoxysilane precursor. Elemental analysis found 14.01% C, 4.90% H, and 0.205% N, corresponding to 0.300 μmol HRP per gram of solid. The enzyme encapsulated in propylated silica glass, designated HRP@$PrSiO_2$, was obtained using 1.9714 g of trimethoxypropylsilane precursor. Elemental analysis found 35.01% C, 15.82% H, and 0.410% N, corresponding to 0.586 μmol HRP per gram of solid. When hexyltrimethoxysilane (2.4761 g) was used as a glass precursor, gelation was very slow, yielding a jelly-like mass even after 10 days of air-drying at 40 °C. This mass dissolved completely upon washing with acetone. When *iso*-butyltrimethoxysilane (2.2057 g) was used as a glass precursor, a soft, creamy solid was obtained after 7 days of air-drying at 40 °C. This solid dissolved almost completely upon washing with acetone.

2.5. Oxidation of ABTS by H_2O_2 catalyzed by horseradish peroxidase

A sample of encapsulated HRP containing 1.500–2.000 nmol of the enzyme was weighed and suspended in an ABTS solution in a quartz cuvette sized 1.000 cm × 1.000 cm × 4.500 cm. Reaction was started by addition of 9.150 mM solution of hydrogen peroxide. Interconversion of ABTS ($\lambda_{max} = 340$ nm) to its radical cation ($\lambda_{max} = 414$ nm) was monitored by taking UV–VIS spectra of reaction mixture every 10 min. In experiments with dissolved enzyme, spectra were taken every 0.5 min.

2.6. Electrochemical oxidation of ABTS

A modification of a published method [14] was used. Solution of ABTS (2.00 mM) in sodium phosphate buffer was subjected to a constant-current electrolysis in a cell containing a platinum working electrode, a platinum reference electrode, and a stainless steel counter electrode. The current was maintained at 10 mA for 30 min.

2.7. Enzymatic over-oxidation of ABTS

To a solution containing HRP (2 nmol) and ABTS (100 nmol) in 3.9385 ml of a phosphate buffer, was added 61.5 μl of aqueous hydrogen peroxide (16.25 mM, 1 μmol). The color of the solution gradually became green, indicating $ABTS^{\bullet+}$ formation, and later pale-yellow, indicating over-oxidation. The transformation of $ABTS^{\bullet+}$ into an oxidized product was followed by UV–VIS spectroscopy; the maximum concentration of this product was reached after 4 h.

2.8. Chemical over-oxidation of ABTS

ABTS (40 μmol) was dissolved in ca. 150 ml of a 50 mM sodium phosphate buffer at pH 6.0. Aqueous ammonium persulfate (4.00 ml of a 1.00 M solution) was added dropwise. The color of the solution immediately became green, indicating $ABTS^{\bullet+}$ formation; and later pale-yellow, indicating over-oxidation. This process was followed by analytical HPLC; it was complete after 1 h. Upon removal of water by rotary evaporation, a yellow oil mixed with a white solid remained. This residue was dissolved in ca. 2.0 ml of water and subjected to preparative HPLC. Five fractions with retention times of 16.0, 19.3, 21.5, 22.5, and 24.1 min were collected, and their UV–VIS spectra were recorded. Upon removal of eluent by rotary evaporation and re-dissolution in D_2O, ^1H and COSY NMR spectra were recorded (see Section 4.1).

3. Results and discussion

3.1. Choice of reaction

HRP [15–18] contains heme with histidine as an axial ligand. A bulky phenylalanine side chain shields the distal side of the heme, that opposite to the axial histidine, and prevents pre-association of the substrate in the hydrophobic pocket of the active site, as in oxidations catalyzed by cytochrome P-450.

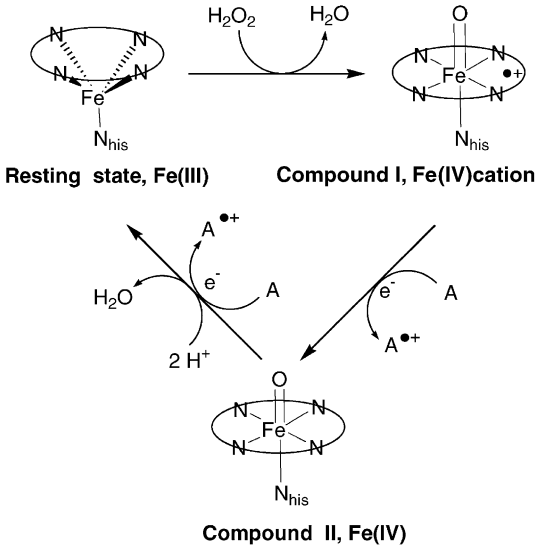

Scheme 1. Peroxidase catalytic cycle: A is the substrate, radical–cation $A^{\bullet+}$ is the product.

Therefore, electron transfer in Scheme 1 occurs via the heme edge.

One- and two-electron oxidation of the dianion ABTS and of the related systems was investigated in the 1960s by Hünig et al. [19–21]. A decade later, ABTS was proposed to serve as a chromogen for hydrogen peroxide assay using HRP, because it has a well-defined absorption maximum at 340 nm ($\varepsilon_{340} = 3.6 \times 10^4\,M^{-1}\,cm^{-1}$) [22]. The radical–cation $ABTS^{\bullet+}$ has an absorption maximum at 414 nm (ε_{414}=$3.6 \times 10^4\,M^{-1}\,cm^{-1}$); it absorbs also at 340 nm ($\varepsilon_{340} = 5.4 \times 10^3\,M^{-1}\,cm^{-1}$) [22]. The ABTS method allows for easy quantification of the initial rates in the enzymatic reaction. Most of the commercially-available peroxidase is now assayed using this method [12]. Because in this study we investigate the effects of the glass matrix on the reactivity of the encapsulated enzyme, we need a well-behaved reaction, whose kinetics can be interpreted with confidence. Oxidation of ABTS by H_2O_2 is such a reaction.

3.2. Preparation and characterization of catalysts

HRP was encapsulated into silica and organosilica glasses by the sol–gel method (Scheme 2). The same batch of the enzyme was used for all encapsulations. The "loading" of the catalyst was calculated from the nitrogen content of the sol–gel glass, determined by the elemental analysis. There are 499 nitrogen atoms in HRP amino acid sequence [23]; molecular weight of the enzyme is ca. 40,000, therefore 17.5% of its weight is nitrogen. Since elemental analysis of all undoped sol–gel matrices yielded 0.00% N, as expected, all nitrogen in the HRP-doped sol–gel glasses comes from the enzyme itself.

3.3. Oxidation of ABTS catalyzed by encapsulated horseradish peroxidase

We studied this reaction at pH 6.0 by varying the concentrations of ABTS and hydrogen peroxide; concentration of encapsulated enzyme was kept at 500 nM. Owing to the high absorbance of ABTS, for the sake of accuracy we kept its concentration below 150 μM. Concentration of H_2O_2 was varied from 0.1 to 10 times that of ABTS.

3.4. Stoichiometry is important

We monitored the change of ABTS and $ABTS^{\bullet+}$ concentration with time. As Fig. 1a shows, when concentration of H_2O_2 was one-half or less than that of

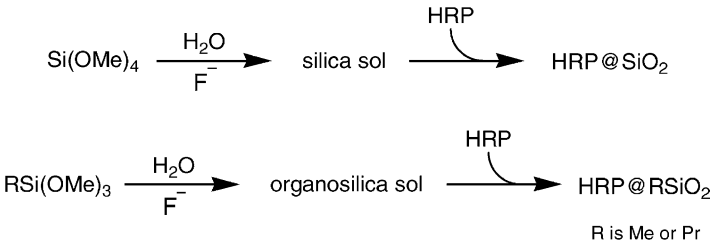

Scheme 2. Encapsulation of horseradish peroxidase (HRP) into silica (top) and organosilica (bottom) sol–gel glass.

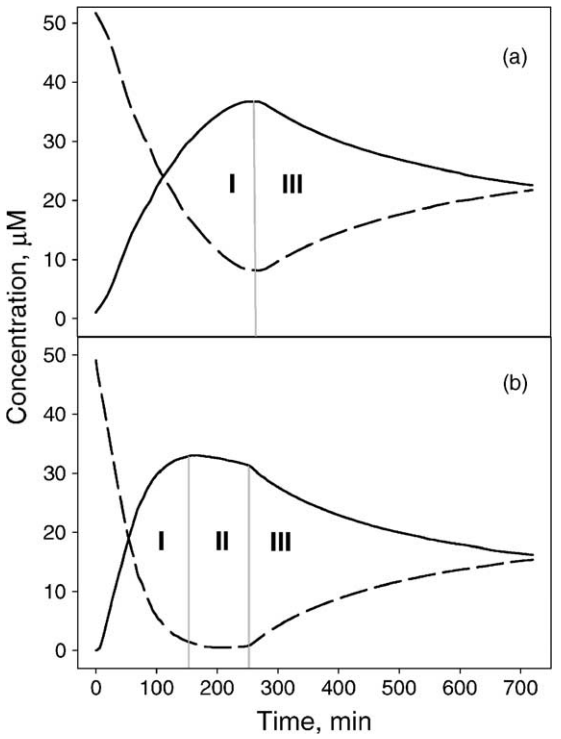

Fig. 1. Effect of H_2O_2 concentration on oxidation of ABTS (dashed lines) into $ABTS^{\bullet+}$ (solid lines) catalyzed by HRP@$MeSiO_2$. Concentration of HRP and initial concentration of ABTS were 500 nM and 50.0 μM, respectively. Initial concentration of H_2O_2 was (a) 25.0 μM, or (b) 50.0 μM i.e. as required by Scheme 1 or twice higher than that.

ABTS, two reactions are seen. In the reaction I, ABTS is converted to $ABTS^{\bullet+}$. In the reaction III, $ABTS^{\bullet+}$ is converted back to ABTS. As Fig. 1b shows, when concentration of H_2O_2 was more than one-half of that of ABTS, in addition to the reactions I and III, there is also reaction II, in which $ABTS^{\bullet+}$ is consumed, while ABTS is not. Reaction I, HRP-catalyzed conversion of ABTS into $ABTS^{\bullet+}$, is the one on which the ABTS assay is based. Reactions II and III can be observed not only for encapsulated, but also for dissolved HRP.

3.5. "Back" reaction

Reaction III, which we call "back reaction", is a conversion of $ABTS^{\bullet+}$ back into ABTS. Little is known about this reaction [14,23], presumably because it is too slow to be detected in the solution assay, which takes less than 10 min. The back reaction, however, becomes important for encapsulated enzymes, where the observed rate of enzyme-catalyzed reaction is limited by the diffusion of the substrate into and the product out of the pores of the sol–gel matrix [4]. Several control experiments support solvent involvement in this re-reduction of $ABTS^{\bullet+}$. (1) When H_2O_2 was eliminated from the reaction mixture by addition of MnO_2, the back reaction continued. (2) When $ABTS^{\bullet+}$ was prepared by electrochemical oxidation of ABTS, the back reaction was observed. (3) Replacement of H_2O solvent with D_2O resulted in a 1.1–2.5-fold decrease in the apparent rate constant of the "back reaction". (4) Lowering pH of the solution, i.e. increasing the H^+ concentration, slows down this reaction [24]. The overall reaction in Eq. (2) agrees with these observations[1]. It is important to note that both enzymatic reaction I and the back reaction III obey the mass-balance requirement, i.e. the sum of ABTS and $ABTS^{\bullet+}$ concentrations remains constant.

$$ABTS^{\bullet+} + \tfrac{1}{2}H_2O \rightarrow ABTS + \tfrac{1}{4}O_2 + H^+ \qquad (2)$$

3.6. Reaction II—over-oxidation of ABTS

Reaction II (Fig. 1b) occurs only in the presence of excess H_2O_2 (i.e., more than 0.5 equivalent with respect to ABTS); it causes disappearance of $ABTS^{\bullet+}$ without its conversion back into ABTS. Instead, the UV bands at ca. 260 and 294 nm grow as the concentration of $ABTS^{\bullet+}$ decreases. UV–VIS spectra of this new product are shown in Fig. 5. We decided to investigate further. The details of this part of our study can be found in Section 4.1. We summarize the findings here.

In the presence of excess of H_2O_2, peroxidase-catalyzed oxidation of ABTS can lead not only to $ABTS^{\bullet+}$, but also further to azodication $ABTS^{2+}$ [13]. The latter is unstable in aqueous solution [24,27,28]; its decomposition products are pale-yellow or colorless. Both chemically [24] and enzymatically [13] generated $ABTS^{2+}$ decompose into the mixture of the same five compounds (Fig. 6). The formation of $ABTS^{2+}$ and of these five by-products can be

[1] The standard potential for the reaction in Eq. (2) is −0.2 V at pH 6.0. It was calculated from known reduction potentials [25] of $ABTS^{\bullet+}$ (+0.67 V) and $ABTS^{2+}$ (+1.07 V) and the oxidation potential of water [26] (+0.874 V at pH 6.0).

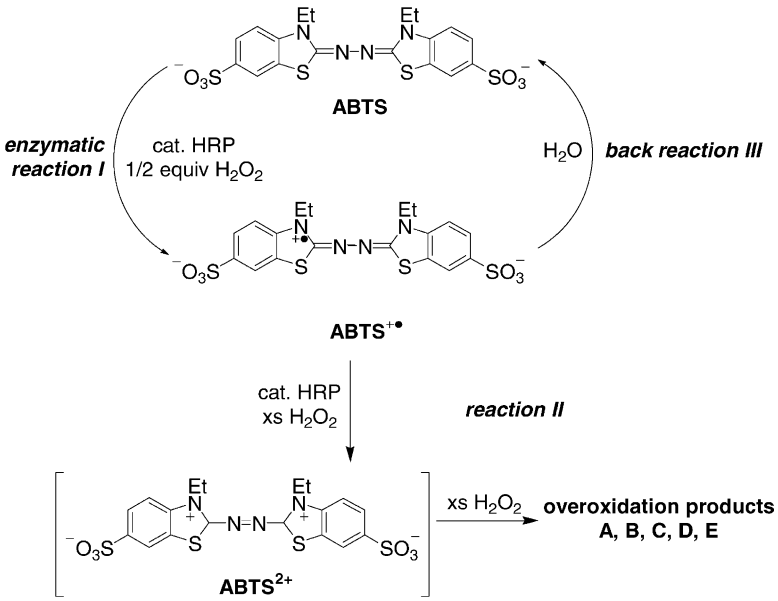

Scheme 3. Oxidation of ABTS by hydrogen peroxide is catalyzed by horseradish peroxidase (HRP) encapsulated in sol–gel silica glass.

avoided by using at most 0.5 equivalent H_2O_2 for each equivalent of ABTS; under these conditions, only the normal peroxidase cycle (shown in Scheme 1) operates. All reactions involved in the oxidation of ABTS by H_2O_2 in the presence of encapsulated HRP are summarized in Scheme 3.

All further experiments in this study were conducted using a 2:1 ratio of ABTS to H_2O_2.

3.7. ABTS oxidation catalyzed by horseradish peroxidase encapsulated in silica and organosilica matrices

After identifying the conditions under which undesirable side-reactions were suppressed, we investigated the effect of matrix on the ABTS oxidation catalyzed by encapsulated enzyme. We determined maximum yield of radical–cation $ABTS^{\bullet+}$ (Fig. 1a, the apex of the $ABTS^{\bullet+}$ trace), and the apparent first-order enzymatic rate constant for reaction I.

As Fig. 2 shows, much higher yields are achieved when the enzyme is encapsulated in $MeSiO_2$ than in SiO_2 and $PrSiO_2$. As the concentration of substrate ABTS is raised, the yield slightly decreases, because more and more turnovers are required from the enzyme.

As Fig. 3 shows, rate constants for the $MeSiO_2$ matrix are ca. 10 and 7 times larger than those for SiO_2 and $PrSiO_2$ matrices, respectively.

This difference in the enzymatic rate constants between SiO_2 and $MeSiO_2$ may be due to the elec-

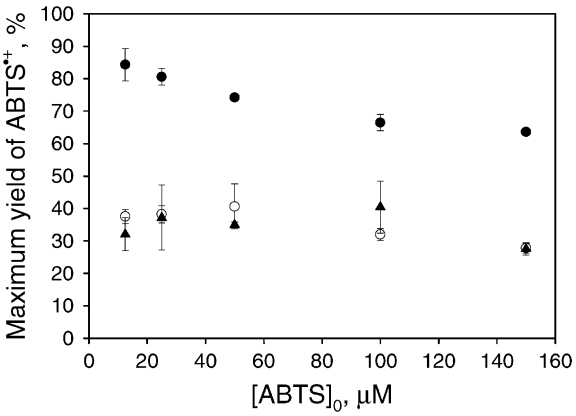

Fig. 2. Dependence of maximum yield of radical cation $ABTS^{\bullet+}$ on initial concentration of ABTS in an oxidation reaction at pH 6.0 catalyzed by horseradish peroxidase encapsulated in silica, designated HRP@SiO_2 (○); methylated silica, designated HRP@$MeSiO_2$ (●); and propylated silica, designated HRP@$PrSiO_2$ (▲). Concentration of the enzyme in all experiments was 500 nM.

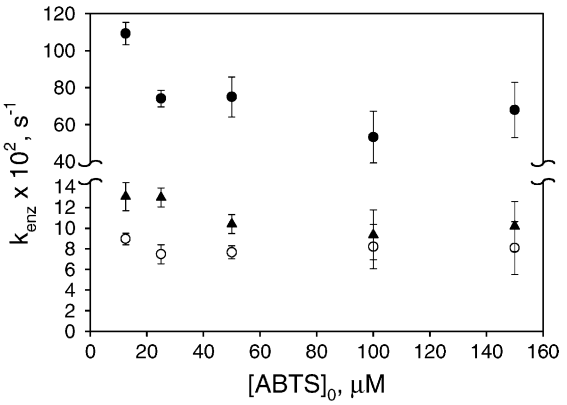

Fig. 3. Apparent enzymatic rate constant k_{enz} for conversion of ABTS into $ABTS^{\bullet+}$ at pH 6.0 as a function of initial concentration of ABTS. This oxidation by H_2O_2 was catalyzed by HRP@SiO_2 (○), HRP@$MeSiO_2$ (●), and HRP@$PrSiO_2$ (▲). Concentration of the enzyme in all experiments was 500 nM.

trostatic repulsion between the negatively-charged substrate, ABTS, and the negatively-charged surface of silica matrix. In order to reach the encapsulated enzyme, substrate must first diffuse through the pores and channels of the matrix. Free silanol groups, which are negatively charged at pH 6.0, are abundant on the surface of silica. The surface of methylated silica contains methyl groups, which are electroneutral.

The $ABTS^{\bullet+}$ yields and the enzymatic rate constants observed with propylated silica, $PrSiO_2$, as the enzyme matrix are closer to the respective parameters for silica than to those for methylated silica, for several possible reasons. First, the non-polarity of propylated silica matrix hinders diffusion of ABTS, the polar substrate. Second, the steric bulk of the propyl substituents may render the polycondensation reaction incomplete, so that some silanol groups, with their negative charge, remain on the matrix surface. The electrostatic repulsion between ABTS and the matrix would again come into play. The first explanation is supported by the existence of an induction period of ca. 120 min for ABTS oxidation catalyzed by HRP@$PrSiO_2$. The second explanation is consistent with the decreasing gelation rate and, thus, decreasing extent of cross-linking [1,28], as the alkyl chain R in the precursors $RSi(OMe)_3$ grows in order Me, Pr, Bu^i, and Hex.

3.8. Effect of the ionic strength on ABTS oxidation in different matrices

To test the hypothesis of electrostatic repulsion, we investigated the dependence of the enzymatic rate constant on the ionic strength of the buffer solution. The ionic strength of our usual 50-mM sodium phosphate buffer is 62 mM. The ionic strength was raised to 562 mM by addition of 0.500 M solution of sodium chloride, or lowered to 2.48 mM by using a 2.00-mM sodium phosphate buffer. The results are shown in Fig. 4. For the enzymatic rate constants obtained with HRP@$MeSiO_2$, there is no dependence on ionic strength. Enzymatic rate constants obtained with HRP@SiO_2 and HRP@$PrSiO_2$ increase more than 2.5-fold upon increase in the ionic strength. These experiments support our electrostatic explanation for the diminished rate constants and yields in ABTS oxidation catalyzed by HRP@SiO_2 and HRP@$PrSiO_2$, in comparison with HRP@$MeSiO_2$.

3.9. Optimal choice of the matrix

The surface of the silica matrix SiO_2 is negatively charged. Methylation of the surface, as in $MeSiO_2$, neutralizes most of the negative charge on the surface. Propylation, as in $PrSiO_2$, lowers the degree of cross-linking or raises the number of free silanol

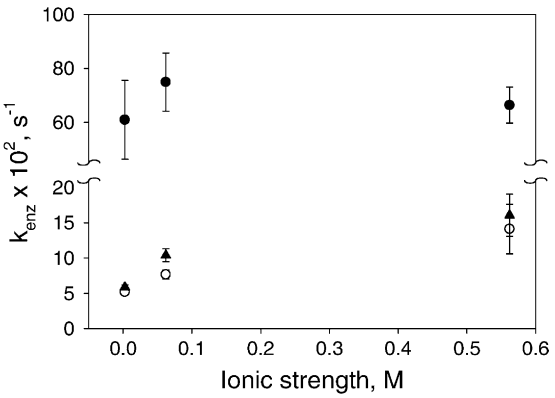

Fig. 4. Apparent enzymatic rate constant k_{enz} for conversion of ABTS into $ABTS^{\bullet+}$ as a function of the ionic strength of the buffer at pH 6.0. ABTS oxidation by H_2O_2 was catalyzed by HRP@SiO_2 (○), HRP@$MeSiO_2$ (●), and HRP@$PrSiO_2$ (▲). Concentration of the enzyme in all experiments was 500 nM; initial concentrations of ABTS and H_2O_2 were 50.0 and 25.0 μM, respectively.

groups on the surface, in comparison with the methylation. Since the substrate ABTS is negatively charged, the highest conversion and apparent enzymatic rate constants are achieved with HRP encapsulated into the methylated silica matrix.

4. Conclusion

This study promotes understanding of encapsulated and otherwise immobilized enzymes. Because the enzyme and the surrounding matrix may interact in various and subtle ways, complications may arise even with common and widely-used assays. Electrostatic effects, absent in solution, can manifest themselves in glass and affect the observed catalytic activity. These effects may be recognized, and even suppressed, by varying the matrix material. All these factors must be taken into consideration in the design of biosensors, supported catalysts, and other composite materials.

4.1. Supporting information

4.1.1. ABTS over-oxidation products

Previous studies mentioned peroxidase-catalyzed formation of $ABTS^{2+}$ from ABTS in the presence of excess of H_2O_2 [13], but UV–VIS spectra of our enzymatic reaction mixtures lacked characteristic absorbance of $ABTS^{2+}$ at ca. 518 nm [25]. Thus, we prepared over-oxidation product in larger amounts, to learn more about it.

We took the conditions of a spectrophotometric experiment in solution (Fig. 5), at which over-oxidation was detected, as a starting point. Preserving the HRP:ABTS:H_2O_2 molar ratio of 1:50:500, we varied concentration of dissolved HRP from 0.5 to ca. 27 μM. However, both the formation and the disappearance of $ABTS^{\bullet+}$ were much slower than those in the spectrophotometric experiment, and over-oxidation product was not detected in the reaction mixture. At such high concentration of hydrogen peroxide, enzyme was deactivated almost instantly. Therefore, scaling up the reaction by increasing the concentrations of all components would not have produced enough over-oxidation product.

If transient $ABTS^{2+}$ was indeed formed during the enzyme-catalyzed oxidation of ABTS by excess of H_2O_2, perhaps the over-oxidation product was formed from $ABTS^{2+}$. Indeed, there are reports of colorless $ABTS^{2+}$decomposition product formed in the presence of excess of oxidant [27,28]. We checked this hypothesis by preparing $ABTS^{2+}$ by chemical oxidation of ABTS.

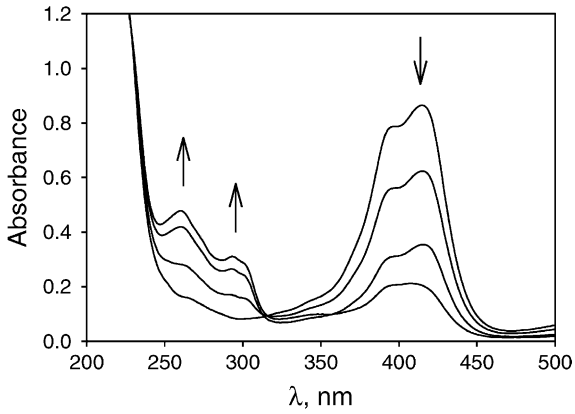

Fig. 5. Conversion of $ABTS^{\bullet+}$ (λ_{max} = 414 nm) into over-oxidation product (λ_{max} = 260 and 294 nm) at pH 6.0. UV–VIS spectra were taken 10 min, 1, 2, and 3 h after the addition of H_2O_2 to the sodium phosphate solution containing HRP and ABTS. Conditions: [HRP] = 500 nM; $[ABTS]_0$ = 25.0 μM; $[H_2O_2]_0$ = 250 μM.

When ABTS was oxidized by an excess of peroxidisulfate ($S_2O_8^{2-}$), $ABTS^{\bullet+}$ and then $ABTS^{2+}$ were formed [24], but the latter quickly decayed, leaving the solution pale-yellow. The UV–VIS spectrum of this almost colorless solution exhibited the characteristic UV-bands earlier observed for enzymatically-obtained over-oxidation product. Encouraged by this result, we optimized the conditions of experiment, to maximize the yield of over-oxidation product. The analytical HPLC traces of over-oxidation product obtained by enzymatic and chemical over-oxidation of ABTS are shown in Fig. 6. In both cases, there are not one, but five compounds. We designate them A through E, in order of their elution from the column.

After preparative HPLC separation of these compounds from the chemically-obtained mixture, their UV–VIS, NMR, and mass spectra were recorded (see Fig. 7 and Tables 1 and 2, respectively). The ^{1}H NMR spectra of all compounds contain signals of the ethyl groups and of 1,3,4-substituted benzene rings, which are present in ABTS itself. ^{1}H NMR spectra of B and E show only one kind of ethyl group and one kind

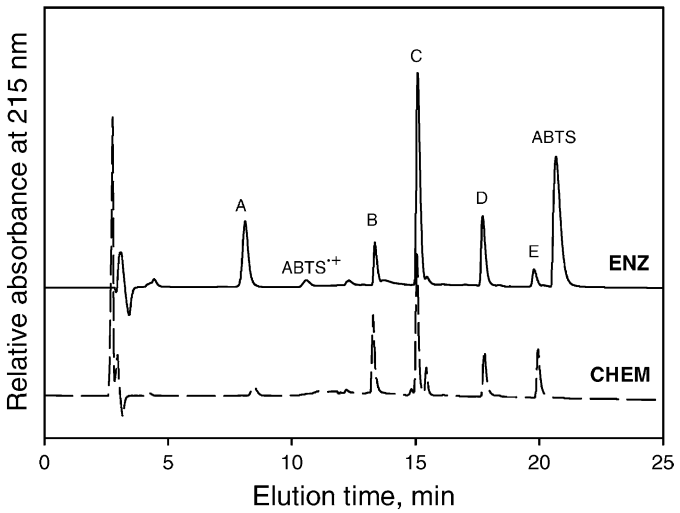

Fig. 6. HPLC traces of the mixtures of over-oxidation products obtained in different ways. ENZ (solid line) resulted from oxidation of ABTS by excess of H_2O_2 in the presence of HRP. CHEM (dashed line) resulted from oxidation of ABTS by excess of $S_2O_8^{2-}$.

of aromatic ring in each of these molecules. Since ABTS molecule has a plane of symmetry, compounds B and E can possess either one or two identical 3-ethylbenzothiazoline groups. Each of the other fractions shows two kinds of ethyl groups and two kinds of aromatic rings. Therefore, compounds A, C, and D each possess two different 3-ethylbenzothiazoline moieties. The ESI–MS of B contains a peak with an *m*/*z* ratio of 258, which is consistent with the molecular mass of 3-ethyl-2-benzothioazolinone-6-sulphoimine.

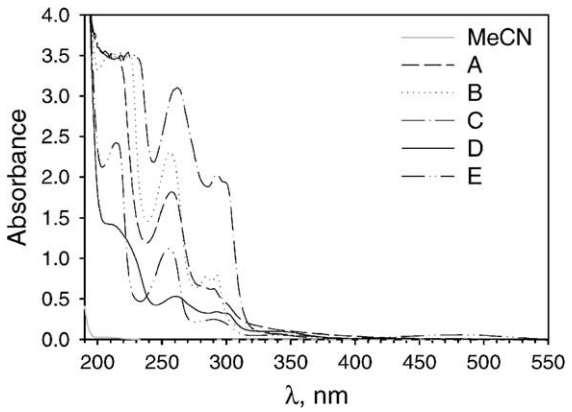

Fig. 7. UV–VIS spectra of compounds A through E. The mixture of over-oxidation products was obtained by oxidation of ABTS by excess of $(NH_4)_2S_2O_8$ (see CHEM trace on Fig. 6); fractions A through E were separated by preparative HPLC. All UV–VIS spectra were recorded with deionized water in the reference cuvette. Since percentage of acetonitrile (MeCN) in an eluent varied, depending on the elution time, a spectrum of pure MeCN is shown for comparison.

Mixtures of several products of ABTS over-oxidation obtained by chemical (peroxidisulfate) or enzymatic (laccase) reactions were also observed [24]. The HPLC traces of each mixture contain several peaks eluting between those of $ABTS^{\bullet+}$ and ABTS. The two largest ones, so-called P_1 and P_2, were proposed to be 3-ethyl-2-benzothioazolinone-6-sulphoimine (the same as our compound B) and 3-ethyl-2-benzthiaxolone-6-sulphonic acid, respectively [24]. However, this proposal was based on the results of a previous study of non-sulfonated ABTS analogs in organic solvents [30].

The findings presented here suggest that in the presence of excess of H_2O_2, HRP-catalyzed oxidation of ABTS leads not only to $ABTS^{\bullet+}$, but also to azodication $ABTS^{2+}$, which in turn decomposes into five compounds. We separated them by HPLC, and designated them A through E. This over-oxidation route can be suppressed by using at most 0.5 equivalent H_2O_2 for each equivalent of ABTS.

For further reading see [29].

Table 1
^{1}H NMR spectra of compounds A through E

Compound	^{1}H NMR signals (400 MHz, D_2O)[a]
A	8.21 (d, $J = 2.0$, 1H), 8.15 (d, $J = 2.0$, 2H), 8.09 (d, $J = 1.3$, 1H), 8.06 (d, $J = 1.7$, 1H), 8.03 (d, $J = 1.9$, 1H), 8.01 (d, $J = 2.2$, 1H), 7.63 (d, $J = 8.5$, 1H), 7.52 (d, $J = 8.9$, 2H), 4.27 (q, $J = 6.9$, 2H), 4.06 (q, $J = 7.1$, 2H), 1.35 (t, $J = 7.2$, 3H), 1.28 (t, $J = 7.0$, 3H)
B	7.90 (d, $J = 1.4$, 1H), 7.77 (dd, $J_1 = 8.6$, $J_2 = 1.6$, 1H), 7.26 (d, $J = 8.4$, 1H), 3.99 (q, $J = 7.2$, 2H), 1.23 (t, $J = 7.2$, 3H)
C	8.23 (s, 1H), 8.13 (d, $J = 9.1$, 1H), 7.84 (s, 1H), 7.77(d, $J = 8.8$, 1H), 7.63 (d, $J = 8.6$, 1H), 7.29 (d, $J = 8.8$, 1H), 4.26 (q, $J = 7.0$, 2 H), 4.17 (q, $J = 6.7$, 1H), 1.37 (t, $J = 7.0$, 3H), 1.32 (t, $J = 7.1$, 3H)
D	8.22 (d, $J = 8.1$, 1H), 8.13 (d, $J = 9.2$, 1H), 7.84 (s, 1H), 7.77 (d, $J = 8.3$, 1H), 7.63 (d, $J = 9.1$, 1H), 7.36 (s, 1H), 7.29 (d, $J = 8.8$, 1H), 4.25 (q, $J = 5.6$, 2H), 4.12 (q, $J = 6.7$, 2H), 1.37 (t, $J = 7.2$, 3H), 1.31 (t, $J = 7.1$, 3H)
E	8.17 (d, $J = 1.6$, 1H), 8.14 (dd, $J_1 = 8.9$, $J_2 = 2.0$, 1H), 7.67 (d, $J = 9.1$, 1H), 4.12 (q, $J = 7.1$, 2H), 1.31 (t, $J = 7.1$, 3H)

[a] Some small splitting constants in the aromatic region could not be determined accurately because of the low concentration of the analytes.

Table 2
Electrospray ionization–mass spectral (ESI–MS) analysis of ABTS, $ABTS^{\bullet+}$, and compounds A through E[a]

Compound	Major ESI–MS peaks, $m/z > 200$[b]
ABTS	**256** (M), 513 ($M + H^+$)
$ABTS^{\bullet+}$	**512** (M)
A	228, 249, 258, 274, 280, **289**, 305
B	**258**, 280, 372
C	258, **280**, 304, 381, 582
D	**249**, 304, 363, 385, 397, 520
E	227, **249**, 385, 521

[a] Data shown were obtained in the negative mode, in the m/z range from 35 to 650 amu.
[b] The peak with the highest intensity is shown in bold.

Acknowledgements

We thank Stephen Veysey for the elemental analyses, Nebojša M. Milović for the HPLC experiments, Brett Simpson for the electrochemical experiment, and Dr. Kamel A. Harrata for the ESI spectra. We are also grateful to Prof. James H. Espenson and Dr. Andreja Bakac for helpful discussions. This research was supported by the National Science Foundation.

References

[1] M.T. Reetz, A. Zonta, J. Simpelkamp, Biotech. Bioeng. 49 (1996) 527.
[2] C. Shen, N.M. Kostić, J. Electroanal. Chem. 438 (1997) 61.
[3] C. Shen, N.M. Kostić, J. Am. Chem. Soc. 119 (1997) 1304.
[4] J.D. Badjić, N.M. Kostić, Chem. Mater. 11 (1999) 3671.
[5] J.D. Badjić, N.M. Kostić, J. Phys. Chem. B 104 (2000) 11081.
[6] J.D. Badjić, N.M. Kostić, J. Mater. Chem. 11 (2001) 404.
[7] J.D. Badjić, N.M. Kostić, J. Phys. Chem. B 105 (2001) 7482.
[8] J.D. Badjić, E.N. Kadnikova, N.M. Kostić, Org. Lett. 3 (2001) 2025.
[9] E.N. Kadnikova, N.M. Kostić, J. Non-Cryst. Solids 283 (2001) 63.
[10] E.H. Lan, B. Dunn, J.S.V. Valentine, J.I. Zink, J. Sol–Gel Sci. Tech. 7 (1996) 109.
[11] L. Zheng, W.R. Reid, J.D. Brennan, Anal. Chem. 69 (1997) 3940.
[12] L. Zheng, J.D. Brennan, Analyst 123 (1998) 1735.
[13] J. Pütter, R. Becker (Eds.), Peroxidases, Vol. 3, 3rd Edition, Verlag Chemie, Deerfield Beach, FL, 1983.
[14] D.P. Barr, S.D. Aust, Arch. Biochem. Biophys. 303 (1993) 377.
[15] P.R. Ortiz de Montellano, Acc Chem. Res. 20 (1987) 289.
[16] H.B. Dunford, J.S. Stillman, Coord. Chem. Rev. 19 (1976) 187.
[17] J.H. Dawson, Science 240 (1988) 433.
[18] A.M. English, G. Tsaprailis, Adv. Inorg. Chem. 43 (1995) 79.
[19] S. Hünig, Liebigs Ann. Chem. 676 (1964) 32.
[20] S. Hünig, H. Balli, H. Conrad, A. Schott, Liebigs Ann. Chem. 676 (1964) 36.
[21] S. Hünig, H. Balli, H. Conrad, A. Schott, Liebigs Ann. Chem. 676 (1964) 52.
[22] R.E. Childs, W.G. Bardsley, Biochem. J. 145 (1975) 93.
[23] K.G. Welinder, Eur. J. Biochem. 96 (1979) 483.
[24] A. Majcherczyk, C. Johannes, A. Huttermann, Appl. Microbiol. Biotechnol. 51 (1999) 267.
[25] S.L. Scott, W.J. Chen, A. Bakac, J.H. Espenson, J. Phys. Chem. 97 (1993) 6710.
[26] CRC Handbook of Chemistry and Physics, 75th Edition, CRC Press, Boca Raton, 1994.
[27] P. Maruthamuthu, L. Venkatasubramanian, P. Dharmalingam, Proc. Indian Acad. Sci. 97 (1986) 213.
[28] P. Maruthamuthu, L. Venkatasubramanian, P. Dharmalingam, Bull. Chem. Soc. Jpn. 60 (1987) 1113.
[29] M.T. Reetz, A. Zonta, J. Simpelkamp, A. Rufinska, B. Tesche, J. Sol–Gel Sci. Tech. 7 (1996) 35.
[30] J. Janata, M.B. Williams, J. Phys. Chem. 76 (1972) 1178.